

Carbon Electrode Endows High-Efficiency Perovskite Photovoltaics Affordable, Fully Printable, and Durable

Gengling Liu, Tian Tian,* Jianyu Yang, Jun-Xing Zhong, Dilbara Gulamova,* and Wu-Qiang Wu*

Perovskite photovoltaics have witnessed overwhelming success over the past decade. Carbon-based perovskite solar cells (C-PSCs), using carbon materials as electrodes, make the perovskite photovoltaics more attractive than ever. Since its first launch in 2013, the development of state-of-the-art C-PSCs has made remarkable achievements in various aspects. Herein, the recent ground-breaking advancement of C-PSCs has been summarized, with a particular focus on highlighting the unique advantages of carbon electrodes that enable perovskite photovoltaics affordable, fully printable, and durable. Limitations and challenges associated with C-PSCs are discussed. An insightful perspective regarding future research directions is provided, revolutionizing the pathway toward new-generation photovoltaics and optoelectronics.

1. Introduction

In recent years, perovskite solar cells (PSCs) have emerged as a new star in the realm of photovoltaics due to their fascinating advantages of high efficiency, low cost, and ease of solution processability.^[1–5] Over the past decade, the PSCs have undergone an unpredictably speedy development, especially regarding power conversion efficiencies (PCEs), with a certified value skyrocketing to 25.7%.^[6] This is already on par with or even higher than that of crystalline silicon solar cells, thus being considered one of the most prospective photovoltaic technologies. The next step toward practical application and commercialization is to realize a perfect balance of the efficiency–stability–cost golden triangle. To date, the high-efficiency PSCs multilayer stack was composed of a charge

transport layer, perovskite layer, and metal counter electrode (CE). It is worth pointing out that the cost of metal CE materials is extremely high, which is even more expensive than the perovskite materials and other functional materials, and hence dominates the fabrication cost of the PSCs.^[7–10] In addition, the metal CEs are normally deposited on top of the device via the thermal evaporation technique, which is complicated and is not compatible with roll-to-roll large-area production. Worse still, the possible chemical reaction between the mobile ions of ionic perovskites and metal CEs would result in undesirable metal electrode corrosion and/or perovskite layer decomposition, especially

under humidity or thermal stress, thus incurring inferior device stability. All above-mentioned disadvantages would undoubtedly limit the long-term deployment and commercialization of perovskite photovoltaics.

The carbon electrodes (i.e., carbon black, graphite, graphene, carbon nanotubes (CNTs), etc.) have been recognized as the most potential alternative CEs for the establishment of low-cost, efficient, and stable PSCs, which can be attributed to the attractive properties of carbon materials themselves, such as low-cost, high-stability, hydrophobicity, high-conductivity, and prominent capability of dissipating heat. More importantly, the carbon electrode is intrinsically inert to ion migration, a great benefit to improve the operational stability of PSCs.^[11,12] In 2013, Han and coworkers first fabricated the PSCs employing carbon electrodes and achieved a PCE of 6.6%.^[13] Since then, the carbon-electrode-based PSCs (C-PSCs) have attracted intensive research interest and have been widely reported. Over the past decade, through rational optimization of compositions, morphologies, processing techniques, contact junctions, and device architectures, the PCEs of C-PSCs have been progressively elevated to exceed 22%,^[14–16] gradually diminishing the PCE gap with the metal CEs-based counterparts. And the operational stability of C-PSCs has been extended to nearly 10 000 h, significantly outperforming the metal CEs-based devices.^[17] In this regard, the C-PSCs seem to be the most ideal option for balancing the cost-efficiency-stability triangle among various kinds of PSCs, thus making the perovskite photovoltaics more prosperous to be commercialized and utilized. Indeed, what other value-added benefits can the carbon electrode-based PSCs (C-PSCs) bring to the community are far more than we could expect, which merits particular attention and profound thinking.^[18]

G. Liu, T. Tian, J. Yang, J.-X. Zhong, W.-Q. Wu
Key Laboratory of Bioinorganic and Synthetic Chemistry (MoE)
Lehn Institute of Functional Materials

School of Chemistry
Sun Yat-sen University
Guangzhou 510006, China
E-mail: tiant59@mail.sysu.edu.cn; wuwq36@mail.sysu.edu.cn

D. Gulamova
Materials Science Institute
SPA “Physics-Sun”
Uzbekistan Academy of Sciences
100084, Uzbekistan
E-mail: gulamova@uzsci.net

 The ORCID identification number(s) for the author(s) of this article can be found under <https://doi.org/10.1002/solr.202200258>.

DOI: 10.1002/solr.202200258

In this perspective, we elaborated on the unique advantages of carbon electrodes, which not only simultaneously improved the efficiency and lifespan of the PSCs, but also enabled the resultant devices affordable, fully printable, and durable. We aimed to highlight the vast potential of C-PSCs toward commercialization. Finally, we discussed the current challenges associated with the C-PSCs and provides an insightful perspective on future research and development direction in this field.

2. The Unique Advantages of Carbon Electrodes in PSCs

2.1. Affordable C-PSCs

The cost of the carbon materials (i.e., USD 20 kg⁻¹ for carbon black) is far lower than that of metals (i.e., USD 60 000/kg for Au), which endow themselves suitable to be applied as CEs in fabricating low-cost PSCs (Figure 1a). Apart from cutting down the cost of CEs, the carbon electrode also showcased a unique advantage to further reduce the fabrication cost by constructing the carrier transport layer (CTL)-free C-PSCs with

ultra-simplified structures. Notably, the widely employed carbon electrode processes an appropriate work function of -5.0 eV, which suits well with the energy level of commonly used perovskites (i.e., MAPbI₃,^[19] (FAPbI₃)_{0.83}(MAPbBr₃)_{0.17},^[20] CsPbI₂Br^[21]), enabling the fabrication of *n-i-p* structured hole transport layer-free (HTL-free) C-PSCs (Figure 1b). More interestingly, the perovskite itself possesses the ability to generate and transport both electrons and holes concurrently because of its ambipolar carrier transport characteristic, and in this case, the implementation of both electron transport layer-free (ETL-free) and HTL-free C-PSCs with the ultra-simplified device structure is highly feasible (Figure 1c).^[22–24] Tang and coworkers first constructed the ultra-simplified PSCs with the structure of FTO/CsPbBr₃/carbon (Figure 1d). To further improve the interfacial charge transfer, both the graphene quantum dots and CsPbBr₂I quantum dots are introduced as interfacial modifiers at the top and bottom interfaces of perovskites, respectively. As a result, the ultra-simplified CTL-free C-PSCs realized a good efficiency of 4.2%, which maintained 80% of its original PCE after operating continuously for 200 h in air.^[25] Very recently, Ma and coworkers synergistically improve the PCE and stability of ultra-simplified CTL-free C-PSCs with a device architecture of FTO/MAPbI₃/carbon via precursor

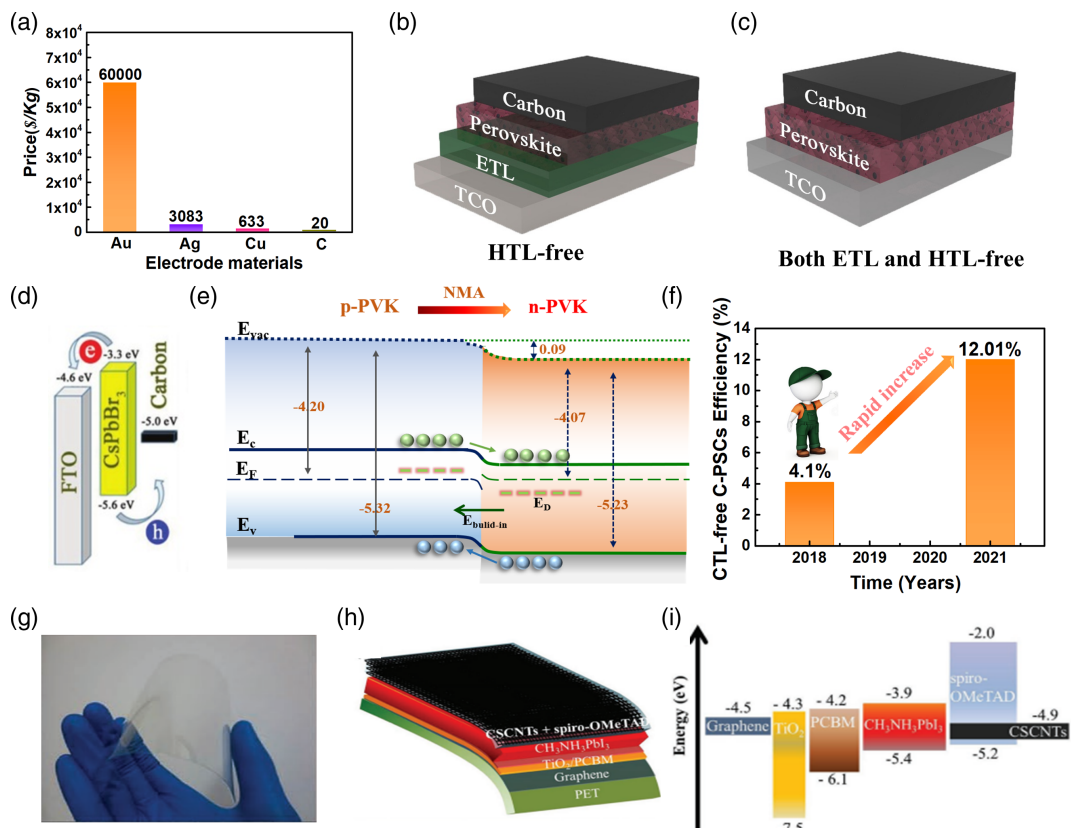


Figure 1. a) A comparison of prices for different electrode materials. Schematic illustration of the carbon-based perovskite solar cells (C-PSCs) with simplified structures: b) Hole transport layer-free (HTL-free) carbon-based device and c) both electron transport layer-free (ETL-free) and HTL-free carbon-based device. d) Schematic energy-levels diagram for CsPbBr₃-based CTL-free C-PSCs. Reproduced with permission.^[25] Copyright 2018, Wiley-VCH. e) A sketch of the energy levels diagram for 1-naphthylmethylamine (NMA)-treated perovskite film showing a favorable n-p homojunction. f) The efficiency evolution for the CTL-free C-PSCs. g) A photograph of graphene/PET conductive substrate. Reproduced with permission.^[27] Copyright 2018, Wiley-VCH. h) Device architecture of the flexible C-PSC using graphene and CNTs and i) its corresponding energy-level diagram. Reproduced with permission.^[27] Copyright 2018, Wiley-VCH.

concentration optimization and additive engineering.^[26] In particular, 0.5 μm thick MAPbI₃ perovskite films with large grains and high crystallinity were fabricated, which ensured sufficient light-harvesting and charge collection, as well as simultaneously reduced the current leakage in the absence of CTL. In addition, incorporation of 1-naphthylmethylamine (NMA) additive was beneficial to further modify the surface of perovskite film, which effectively passivated the surface defects, achieved n-type doping effect (corresponding to up-shifted Fermi level) in perovskite film to form a favorable n-p homojunction with carbon electrode, thus facilitating the hole extraction from doped perovskite layer to carbon electrode (Figure 1e). Consequently, the ultra-simplified device achieved an improved PCE up to 12.01% (Figure 1f), accompanied by a considerably good ambient stability for more than two months. It is worth pointing out that CTL-free C-PSCs configurations can not only minimize the processing complexity but also save the cost for the CTL materials, which could eventually make C-PSCs more affordable. In another case, the carbon electrodes can be fabricated to be transparent and conductive enough, so that it can serve as the substitution of expensive FTO or ITO substrate to assemble the all-carbon electrode-based PSCs with extremely low cost (Figure 1g,h,i).^[16,27]

2.2. Fully Printable C-PSCs

In general, the commonly employed metal CEs are deposited via thermal evaporation, which is time-consuming and limits the up-scaling potential of PSCs. In contrast, the carbon electrodes are easily prepared by solution-based approaches, such as blade-coating or screen printing, which greatly simplifies the production process of PSCs. Other functional layers including

CTLs and perovskite layers can also be fabricated via a solution method, so that fully printable devices can be realized, which is compatible to achieve large-scale, high-throughput, roll-to-roll coating and manufacturing of perovskite photovoltaic devices, thus offering a promising prospect for the future commercialization. Han and coworkers successfully demonstrated the fabrication of HTL-free C-PSCs with successively printed mesoporous TiO₂, ZrO₂, and carbon layers. In their work, the perovskite ink was dropped and penetrated into the perforated TiO₂/ZrO₂/C triple layer-stacking structure. Through the rational design of perovskite compositions and perovskite-additive interaction, the PCEs based on TiO₂/ZrO₂/C mesoporous PSCs improved from 12.84% to 17.68%.^[28–32] Unfortunately, one needs to carefully control the infiltration process of perovskite ink, in which the crystallization of perovskite crystals and the contact between perovskites and other active layers should be carefully optimized.

In fact, it has been widely demonstrated that high-quality, uniform perovskite layers can be fabricated by the means of blade-coating or slot-die coating,^[33] forming intimate contact with adjacent functional layers and making the fully printable PSCs feasible and practical. We for the first time demonstrated a new class of all carbon-based PSCs via layer-by-layer blade-coating of C₆₀ ETL, perovskite absorber, and carbon electrode (Figure 2a). However, the solution-printed C₆₀ layer is not uniform and dense enough, which is not able to guarantee high carrier mobility and conductivity for extracting and effectively transporting electrons. Worse still, the compactness of solution-printed C₆₀ ETL is trendily destroyed by the solvent of perovskite ink, which results in undesirable current leakage or even short-circuiting of PSCs. Given this, we smartly introduced a (3-aminopropyl triethoxysilane (APTES)) ‘molecular

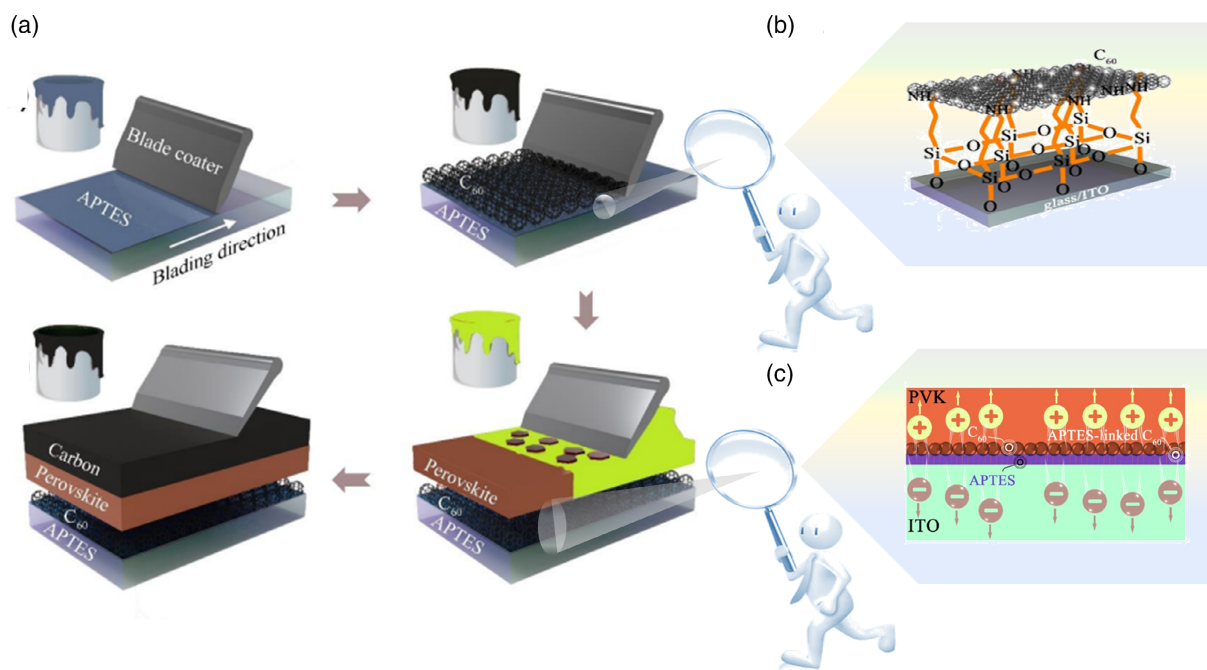


Figure 2. a) Schematic diagram of layer-by-layer blade-coating of carbon-based PSCs with a device structure of ITO/3-aminopropyl triethoxysilane (APTES)-linked C₆₀/perovskite/carbon. b) A sketch showing the APTES-linked C₆₀ on ITO glass. c) Schematic of charge transfer at the APTES-linked C₆₀/perovskite interface. Adapted with permission.^[34] Copyright 2021, Wiley-VCH.

glue' between ITO and C₆₀ layer (Figure 2b).^[34] APTES molecules can be linked at the ITO/ETL interface via strong interfacial connections, maintaining the integrity of the C₆₀ ETL during perovskite deposition, further facilitating the interfacial charge carrier extraction at the ITO/APTES-linked C₆₀/perovskite interface (Figure 2c). Consequently, the full solution-printed HTL-free C-PSCs (ITO/APTES-linked C₆₀/perovskite/carbon) showed a champion efficiency value of 18.64%, which is 77.2% higher than that of the reference device based on pristine C₆₀ ETL without any modification. Overall, the full-solution, layer-by-layer blade-coating can accommodate to scale-up for batch and/or high-throughput fabrication of various perovskite-based optoelectronics. In some cases, the solution-printed carbon electrode was made and engineered as the separated conductive substrate or free-standing film,^[14,35] which was clipped with or adhered on another half-cell. Obviously, the development and implementation of the above-mentioned layer-by-layer printing of monolithic devices are more promising, just like printing the newspaper/magazine in a fast manner.

2.3. Durable C-PSCs

The academic and industrial community have raised a serious concern about the inferior stability of the PSCs, because the perovskite materials are notoriously sensitive to moisture, heat, and light, which can rapidly degrade under harsh conditions.^[36–38] For the high-performance PSCs, the metal CEs might not be the final solutions for making long-life products, since the interdiffusion of metal ions and mobile ions in perovskites would accelerate the decomposition of perovskites and induce metal corrosion, thus deteriorating the device performance.^[39,40] The conductive carbon materials themselves are naturally hydrophobic, which is very suitable to serve as both the top electrode and encapsulation skin of the device. In this case, the carbon electrode serves as the "protection tent" that inhibits the penetration of water (Figure 3a). For our demonstrated HTL-free all carbon-based PSCs without encapsulation, there is almost no decay for all photovoltaic parameters even after storage in a humidity environment with RH of ≈30–50% for 3000 h (Figure 3b).

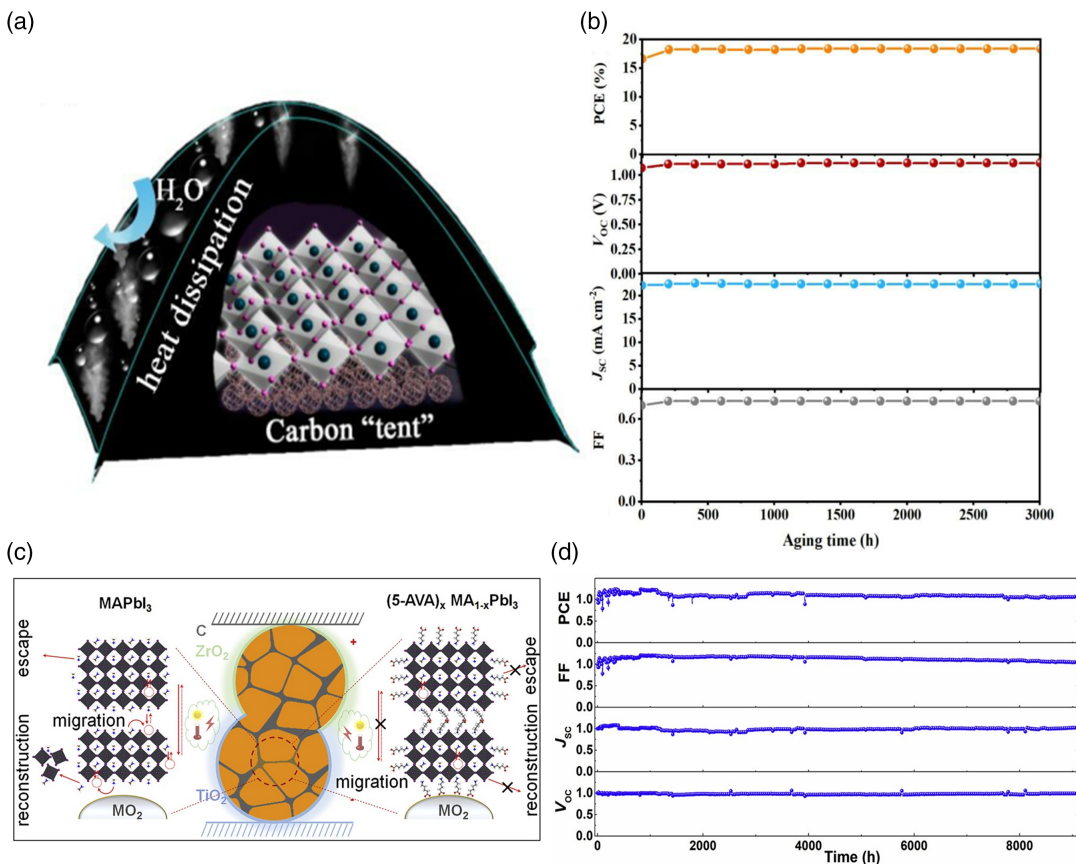


Figure 3. a) Schematic diagram of the carbon tent-assisted protection of perovskite layer that repels the water and releases heat. Reproduced with permission.^[34] Copyright 2021, Wiley-VCH. b) A trace of photovoltaic parameters (power conversion efficiency (PCE), V_{oc} , J_{sc} , and FF) for the PSC fabricated with APTES-modified C₆₀ ETL and carbon electrode when stored in ambient air. Reproduced with permission.^[34] Copyright 2021, Wiley-VCH. c) Schematic showing the (5-ammoniumvaleric acid) 5-AVA-induced nanoconfinement effect in MAPbI₃, which mitigates ion migration and retards material decomposition under the stress of light, heat, and bias. Reproduced with permission.^[17] Copyright 2020, Elsevier Inc. d) 9000-hours maximum power point (MPP) tracking of a printable mesoscopic C-PSC with (5-AVA)_xMA_{1-x}PbI₃. Reproduced with permission.^[17] Copyright 2020, Elsevier Inc.

In addition, the temperature of operating photovoltaic devices is involuntarily increased under continuous illumination, particularly in the scorching summer.^[41,42] The superior thermal conduction and heat dissipation of carbon electrodes can assist in further enhancing the thermal stability of the C-PSCs, enabling them to work stably under elevated temperatures. Furthermore, the chemically inert carbon electrodes could largely mitigate the ions diffusion-triggered electrode corrosion perovskite layer decomposition and device performance degradation. Even so, the presence of mobile ions and/or various types of vacancies defects in perovskites would lead to undesired carrier recombination, especially under continuous operation, which is adverse to the device performance and raises a threat to the long-term stability of PSCs. Very recently, Priya and coworkers introduced perfluorotetradecanoic acid (PFTeDA) with the CO groups and C–F bonds into perovskites for simultaneously passivating the defects and inhibiting ion migration.^[19] Due to the chelation between CO groups of PFTeDA and uncoordinated Pb²⁺ ions, the surface defects are greatly reduced and ion migration is largely suppressed in perovskites. Consequently, the HTL-free C-PSCs with an architecture of FTO/SnO₂/MAPbI₃/carbon reached a commendable efficiency of 18.9%, maintaining 94% of its initial efficiency after being stored for more than one year in ambient air. Han and colleagues used the bifunctional 5-ammoniumvaleric acid (5-AVAI) to stabilize the perovskite grain boundaries via a robust chemical interaction between 5-AVAI and MAPbI₃. The nano-confinement effect induced by 5-AVAI restricts ion migration in perovskites and across the device interface (Figure 3c), greatly contributing to prolonging the operational lifespan of C-PSCs. Combining the excellent long-time stability of carbon electrodes, there is no significant decay when the device was tracked under maximum power point

(MPP) condition for more than 9,000 h (Figure 3d), representing one of the most stable PSCs under operational conditions reported to date.^[12]

3. Conclusion and Outlook

In conclusion, the employment and development of carbon electrodes have brought several fascinating benefits to construct efficient and stable C-PSCs in a low-cost manner. Obviously, this aligns well with the goal of achieving a balanced trade-off in efficiency-stability-cost relationship toward practical commercialization. It deserves to mention that the C-PSCs and metal CEs-based PSCs are not on the same racing track. Obviously, the cost advantage, the full-solution printability, and the extraordinary stability of C-PSCs are incomparable. Though these aspects are promising, there is still a realistic challenge associated with C-PSCs, which is to further improve the PCEs and narrow their gap with metal CEs-based devices, especially for the ultra-simplified devices. The future research directions related to this promising field are as follows (Figure 4).

First, as the intimate partner of the carbon electrode, the quality and optoelectronic properties of the perovskites (i.e., composition, morphology, thickness, crystallinity, crystal orientation, energy level, doping level, conductivity, carrier diffusion length, etc.) should be carefully optimized. In particular, the pin-hole-free perovskite film with suitable thickness is indispensable to construct the CTL-free C-PSCs. Rational doping or additive engineering is required to ensure sufficient carrier conductivity of the perovskite layer. The energy-level alignment between the perovskite layer and carbon electrode should be carefully optimized, and ideally, with favorable interfacial band

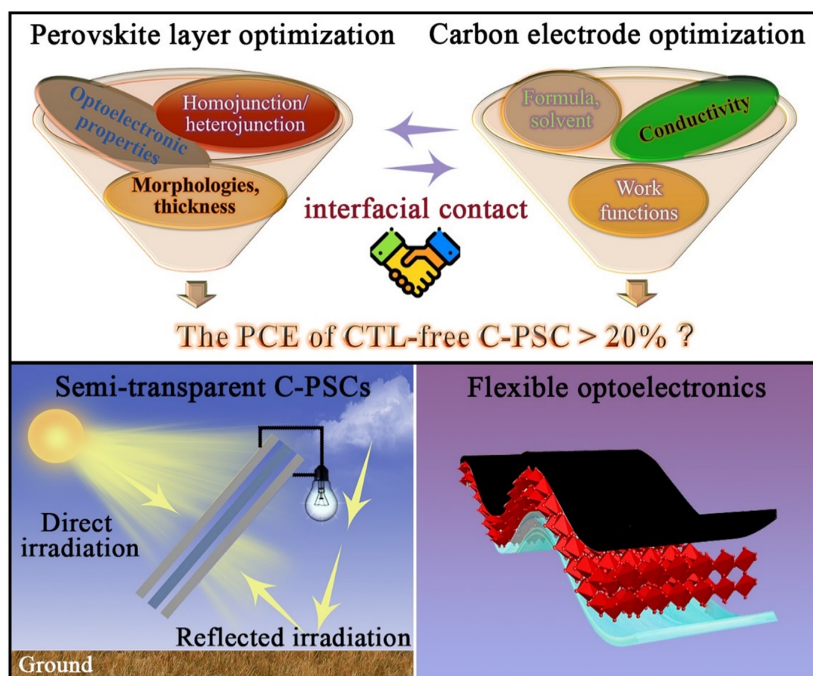


Figure 4. Sketch showing the intermarriage between carbon electrodes and perovskite layers, as well as future research implications and directions for carbon-based perovskite optoelectronic devices.

bending to facilitate the charge extraction and collection. One can also consider employing the perovskite single-crystal thin film with different compositions or constructing the perovskite-perovskite homojunction (i.e., n/n⁺, p/p⁺) to further facilitate the charge separation in the perovskite layer and improve the performance of ultra-simplified C-PSCs.

Second, numerous efforts should be invested in further tuning the ingredients of carbon electrodes, aiming to further improve the conductivity and uniformity of carbon electrodes, as well as altering their work functions to match well with the energy bands of perovskites. In addition to the ingredients, the morphological structures of carbon materials should also be considered.^[43] In this case, the purpose of designing specific carbon structures should be dependent on the specific requirements or functions of the resultant PSCs, including self-encapsulation effect, flexibility, robust mechanical strength, double-sided transparency, etc. The commonly used carbon black nanoparticles possess excellent bonding strength, and normally require thick layer stacking for ensuring considerable conductivity and inducing self-encapsulation effect. The flake-like graphite exhibits good electrical conductivity, but its packing orientation should be carefully controlled, i.e., parallel to the perovskite layer, for the sake of improving the interfacial contact junction and thus charge collection. In addition to the 0D and 2D carbon structures, the 1D CNTs showcased several advantages of small size, good flexibility, and high electrical conductivity, which have been regarded as one of the most promising candidates to fabricate carbon electrodes with good interconnectivity, high transparency, robust mechanical strength, and fast charge transfer tunnel. Tailoring the solvents of homemade carbon paste would be a promising direction to enhance the compatibility of carbon electrodes deposited on the perovskite layer, which would not decompose the perovskite layer during carbon electrode fabrication. And the development of processing techniques is beneficial to strengthen the interfacial point-to-point contact between perovskite crystals and carbon materials, which is pivotal to lifting up the fill factor of the C-PSCs, ideally more than 80%. The synergistic optimization of the perovskite layer, carbon electrode, and their mutual interface is possible to further improve the PCEs of the CTL-free C-PSCs by over 20%.

Third, the carbon electrodes can be engineered to have considerable transparency via carbon-network design, while maintaining sufficient conductivity. It is worth pointing out that the main challenges for practical bifacial C-PSCs lie in achieving balanced light-harvesting and photovoltaic performance, regardless of front- or rear-side illumination. Integrating the bifacial devices with the smart solar tracker will help to maximize the light-harvesting efficiency. One also needs to carefully consider the light transmittance, absorption, reflection, and scattering behaviors at different electrodes and interfaces with mutual interference, and pay particular attention to mitigating the differentiated diffusion lengths of photoexcited carriers in perovskites with different compositions. This could provide a new opportunity to design a variety of new classes of photovoltaic devices, such as semitransparent bifacial C-PSCs, multi-terminal perovskite-based tandem cells, etc.

Last but not least, other potential and unique advantages of carbon electrodes should be further explored, for instance, extending their application to other perovskite-based

optoelectronic devices, such as detectors or X-Ray imagers. We anticipated that the concept of C-PSCs can be embodied in different forms, like plastic devices or fiber-shaped devices for wearable self-powering electronics.

Acknowledgements

The authors acknowledge the financial support from the National Natural Science Foundation of China (22005355) and Guangdong Basic and Applied Basic Research Foundation (2019A1515110770).

Conflict of Interest

The authors declare no conflict of interest.

Keywords

carbon materials, low-cost, perovskite solar cells, solution processability, stability

Received: March 22, 2022

Revised: April 11, 2022

Published online: May 1, 2022

- [1] M. J. P. Alcocer, T. Leijtens, L. M. Herz, A. Petrozza, H. J. Snaith, *Science* **2013**, 342, 341.
- [2] V. Adinolfi, W. Peng, G. Walters, O. M. Bakr, E. H. Sargent, *Adv. Mater.* **2018**, 30, 1700764.
- [3] J.F. Liao, W. Q. Wu, Y. Jiang, J. X. Zhong, L. Wang, D.B. Kuang, *Chem. Soc. Rev.* **2019**, 49, 354.
- [4] H. Kanda, V. D. Mihailescu, M.-E. G. Farret, J.-P. Kleider, Z. Djebbour, J. Alvarez, B. Philippe, O. Isabella, M. R. Vogt, R. Santbergen, P. Schulz, F. Peter, M. K. Nazeeruddin, J. P. Connolly, *Interdiscipl. Mater.* **2022**, 1, 148.
- [5] Y. Mo, C. Wang, X. Zheng, P. Zhou, J. Li, X. Yu, K. Yang, X. Deng, H. Park, F. Huang, Y.-B. Cheng, *Interdiscipl. Mater.* **2022**, <https://doi.org/10.1002/idm2.12022>.
- [6] NREL, *National Renewable Energy Laboratory Best Research Cell Efficiency Chart*, <https://www.nrel.gov/pv/cell-efficiency>. (accessed: April 2022).
- [7] H. Back, G. Kim, J. Kim, J. Kong, T. K. Kim, H. Kang, H. Kim, J. Lee, S. Lee, K. Lee, *Energy Environ. Sci.* **2016**, 9, 1258.
- [8] W. Q. Wu, Q. Wang, Y. Fang, Y. Shao, S. Tang, Y. Deng, H. Lu, Y. Liu, T. Li, Z. Yang, A. Gruverman, J. Huang, *Nat. Commun.* **2019**, 9, 1.
- [9] W. Q. Wu, J. F. Liao, J. X. Zhong, Y. F. Xu, L. Wang, J. Huang, *Angew. Chem., Int. Ed.* **2020**, 132, 21166.
- [10] W. Feng, J. F. Liao, M. Yang, J. X. Zhong, B. X. Lei, L. Ding, W. Q. Wu, *Sol. RRL* **2021**, 5, 2000664.
- [11] M. Hadadian, J. H. Smått, J. C. Baena, *Energy Environ. Sci.* **2020**, 13, 1377.
- [12] G. Tong, T. Chen, H. Li, W. Song, Y. Chang, J. Liu, L. Yu, J. Xu, Y. Qi, Y. Jiang, *Sol. RRL* **2019**, 3, 1900030.
- [13] Z. Ku, Y. Rong, M. Xu, T. Liu, H. Han, *Sci. Rep.* **2013**, 3, 1.
- [14] C. Zhang, S. Liang, W. Liu, F. T. Eickemeyer, X. Cai, K. Zhou, J. Bian, H. Zhu, C. Zhu, N. Wang, Z. Wang, J. Zhang, Y. Wang, J. Hu, H. Ma, C. Xin, S. M. Zakeeruddin, M. Grätzel, Y. Shi, *Nat. Energy* **2021**, 6, 1154.
- [15] H. Zhang, Y. Li, S. Tan, Z. Chen, K. Song, S. Huang, J. Shi, Y. Luo, D. Li, Q. Meng, *J. Colloid Interface Sci.* **2022**, 608, 3151.

- [16] C. Zhang, M. Chen, F. Fu, H. Zhu, T. Feurer, W. Tian, C. Zhu, K. Zhou, S. Jin, S. M. Zakeeruddin, A. N. Tiwari, N. P. Padture, M. Grätzel, Y. Shi, *Energy Environ. Sci.* **2022**, *15*, 1536.
- [17] A. Mei, Y. Sheng, Y. Ming, Y. Hu, Y. Rong, W. Zhang, S. Luo, G. Na, C. Tian, X. Hou, Y. Xiong, Z. Zhang, S. Liu, S. Uchida, T. W. Kim, Y. Yuan, L. Zhang, Y. Zhou, H. Han, *Joule* **2020**, *4*, 2646.
- [18] R. L. McCreery, *Chem. Rev.* **2008**, *108*, 2646.
- [19] T. Ye, Y. Hou, A. Nozariasbmarz, D. Yang, J. Yoon, L. Zheng, K. Wang, K. Wang, S. Ramakrishna, S. Priya, *ACS Energy Lett.* **2021**, *6*, 3044.
- [20] C. Zhang, S. Wang, H. Zhang, Y. Feng, W. Tian, Y. Yan, J. Bian, Y. Wang, S. Jin, S. M. Zakeeruddin, M. Grätzel, Y. Shi, *Energy Environ. Sci.* **2019**, *12*, 3585.
- [21] J. Du, J. Duan, X. Yang, Y. Duan, Q. Zhou, Q. Tang, *Angew. Chem., Int. Ed.* **2021**, *60*, 10608.
- [22] H. Chen, S. Yang, *Adv. Mater.* **2017**, *29*, 1603994.
- [23] H. Chen, S. Yang, *J. Mater. Chem. A* **2019**, *7*, 15476.
- [24] S. Maniarasu, T. B. Korukonda, V. Manjunath, E. Ramasamy, M. Ramesh, G. Veerappan, *Renew. Sustain. Energy Rev.* **2018**, *82*, 845.
- [25] J. Duan, Y. Zhao, B. He, Q. Tang, *Small* **2018**, *14*, 1704443.
- [26] L. Wang, S. Yang, Q. Han, F. Yu, H. Zhang, X. Cai, C. Zhang, L. Gao, T. Ma, *ChemSusChem* **2021**, *14*, 4776.
- [27] Q. Luo, H. Ma, Q. Hou, Y. Li, J. Ren, X. Dai, Z. Yao, Y. Zhou, L. Xiang, H. Du, H. He, N. Wang, K. Jiang, H. Lin, H. Zhang, Z. Guo, *Adv. Funct. Mater.* **2018**, *18*, 1706777.
- [28] A. Mei, X. Li, L. Liu, Z. Ku, T. Liu, Y. Rong, M. Xu, M. Hu, J. Chen, Y. Yang, M. Grätzel, H. Han, *Science* **2014**, *345*, 295.
- [29] D. Zhang, P. Jiang, D. Li, S. Li, J. Qi, X. Wang, Y. Hu, Y. Rong, A. Mei, H. Han, *Sol. RRL* **2022**, *6*, 2100851.
- [30] X. Chen, Y. Xia, Z. Zheng, X. Xiao, C. Ling, M. Xia, Y. Hu, A. Mei, R. Cheacharoen, Y. Rong, H. Han, *Chem. Mater.* **2022**, *34*, 728.
- [31] X. Chen, Y. Xia, Q. Huang, Z. Li, A. Mei, Y. Hu, T. Wang, R. Cheacharoen, Y. Rong, H. Han, *Adv. Energy Mater.* **2021**, *11*, 2100292.
- [32] J. Du, C. Qiu, S. Li, W. Zhang, W. Zhang, Y. Wang, Z. Qiu, Q. Wang, K. Yang, A. Mei, Y. Rong, Y. Hu, H. Han, *Adv. Energy Mater.* **2021**, *12*, 2102229.
- [33] W. Q. Wu, P. N. Rudd, Q. Wang, Z. Yang, J. Huang, *Adv. Mater.* **2020**, *32*, 2000995.
- [34] T. Tian, J. X. Zhong, M. Yang, W. Feng, C. Zhang, W. Zhang, Y. Abdi, L. Wang, B. X. Lei, W. Q. Wu, *Angew. Chem., Int. Ed.* **2021**, *133*, 23928.
- [35] H. Zhang, J. Xiao, J. Shi, H. Su, Y. Luo, D. Li, H. Wu, Y.-B. Cheng, Q. Meng, *Adv. Funct. Mater.* **2018**, *28*, 1802985.
- [36] B. Philippe, B.W. Park, R. Lindblad, J. Oscarsson, S. Ahmadi, E. M. J. Johansson, H. Rensmo, *Chem. Mater.* **2015**, *27*, 1720.
- [37] N. Aristidou, I. Sanchez-Molina, T. Chotchuangchutchaval, M. Brown, L. Martinez, T. Rath, S. A. Haque, *Angew. Chem., Int. Ed.* **2015**, *54*, 8208.
- [38] H. S. Kim, J. Y. Seo, N. G. Park, *ChemSusChem* **2016**, *9*, 2528.
- [39] L. Liu, S. Huang, Y. Lu, P. Liu, Y. Zhao, C. Shi, S. Zhang, J. Wu, H. Zhong, M. Sui, H. Zhou, H. Jin, Y. Li, Q. Chen, *Adv. Mater.* **2018**, *30*, 1800544.
- [40] L. L. Jiang, Z. K. Wang, M. Li, C. C. Zhang, Q. Q. Ye, K. H. Hu, D. Z. Lu, P. F. Fang, L. S. Liao, *Adv. Funct. Mater.* **2018**, *28*, 1705875.
- [41] J. W. Lee, Z. Dai, T. H. Han, C. Choi, S. Y. Chang, S. J. Lee, N. De Marco, H. Zhao, P. Sun, Y. Huang, Y. Yang, *Nat. Commun.* **2018**, *9*, 3021.
- [42] G. Zhang, P. Xie, Z. Huang, Z. Yang, Z. Pan, Y. Fang, H. Rao, X. Zhong, *Adv. Funct. Mater.* **2021**, *31*, 2011187.
- [43] M. Que, B. Zhang, J. Chen, X. Yin, S. Yun, *Mater. Adv.* **2021**, *2*, 5560.